International Journal of Thermophysics, Vol. 28, No. 2, April 2007 (© 2007)
DOI: 10.1007/s10765-007-0186-y

Measurements of Specific Heat Capacity of Gaseous R-143a Using a Flow Calorimeter

N. Kagawa,[1,2] A. Matsuguchi,[1] and K. Watanabe[3]

The isobaric specific heat capacity (c_p) was measured for R-143a (1,1,1-trifluoroethane) in the gas phase. Ten measurements for R-143a were obtained at temperatures from 311 to 343 K and at pressures from 1.6 to 2.4 MPa. Some of them are close to the saturation curve. The expanded uncertainty ($k = 2$) of the temperature measurements is estimated to be less 25 mK, and that of the pressure measurements is less 8 kPa. The expanded uncertainty for c_p is estimated to range from 9 to 32 $J \cdot kg^{-1} \cdot K^{-1}$. Also, the experimental data were evaluated with available equations of state.

KEY WORDS: equation of state; flow calorimeter; gas phase; isobaric heat capacity; R-143a, 1,1,1-trifluoroethane.

1. INTRODUCTION

In order to develop a reliable equation of state for a fluid, various thermodynamic property measurements of the fluid are required. Among them, isobaric heat capacity (c_p) measurements in the gas phase provide a very useful check for calculations of the second derivative of the specific volume with respect to temperature, which is essential information to develop equations of state, but is challenging to measure accurately. R-143a (1,1,1-trifluoroethane, CH_3CF_3) is used as one component of important alternative refrigerant mixtures, e.g., R-404A and R-507C. However, calorimetric property data for R-143a in the gas phase are very limited.

[1] Department of Mechanical Systems Engineering, National Defense Academy, Yokosuka 239-8686, Japan.
[2] To whom correspondence should be addressed. E-mail: kagawa@nda.ac.jp
[3] Department of System Design Engineering, Faculty of Science and Technology, Keio University, Yokohama 223-8522, Japan.

Mukoyama [1], Mukoyama et al. [2], Nakashima [3], Takei [4], Yasumoto and Watanabe [5], and Yasumoto [6] of Keio University measured 17 points of c_p of R-143a in the gas phase by using a flow calorimeter. But, most of the data have not been published yet. To extend them to near the saturation curve, the apparatus was transferred to our laboratory at the National Defense Academy in 2003.

In this work, we report c_p for R-143a at temperatures from 311 to 341 K, on isobars of 1.6, 1.8, 2.0, 2.2, and 2.4 MPa. These results and the previous data are evaluated with various equations of state.

2. MEASUREMENTS

2.1. Experimental Procedure

A flow calorimeter (D in Fig. 1) was used for these measurements; it has been described previously in detail by Mukoyama et al. [2]. A stable and steady flow of sample gas is provided, and a heat flux is generated by a microheater inserted in the calorimeter tube. The calorimeter tube is surrounded with an evacuated thermal shield, and the tube and shield are placed in a well-stirred water bath which is controlled at the target temperature within ±10 mK. Each c_p point is determined by measuring the temperature increment, ΔT, and mass flow rate, $\dot{m}$, of R-143a.

To measure the temperature increment, two calibrated standard platinum resistance thermometers (PRTs) (P1, P2) are located at both ends of the microheater in the sample flow. To measure the mass flow rate, a three-way solenoid valve (K), a timer (L), and a sampling cylinder (I) were used. During 1 min, the sample flowed into the cylinder that was cooled by liquid nitrogen. The cylinder mass was measured with an electronic balance (the uncertainty is 0.1 mg). To establish a stable sample flow in the calorimeter tube during measurements, a condenser (M) with a liquid pump (N), an evaporator (B), and a nozzle (needle valve) (G) are used for the apparatus. The liquid pump which is a bellows type driven by a stepping motor, was developed by Nakashima [3]. The fluctuations of the sample flow ($\dot{m}_{\mathrm{fluc}}/\dot{m}$) were usually less ±0.5%, but the maximum reached ±2.3%. For this study, a mass flow meter (R) was inserted after the sampling cylinder to observe the flow conditions. The mass flow can be adjusted by the needle valve (G).

By measuring the heat input to the heating element, $\dot{Q}$, and mass flow rate, experimental values of $c_{p\mathrm{app}}$ are obtained from

$$c_{p\mathrm{app}} = \frac{\dot{Q}}{\dot{m}\Delta T} = \frac{\dot{Q}_{\mathrm{R}}}{\dot{m}\Delta T} + \frac{\dot{Q}_{\mathrm{L}}}{\dot{m}\Delta T} = c_p + \frac{\dot{Q}_{\mathrm{L}}}{\dot{m}\Delta T}. \tag{1}$$

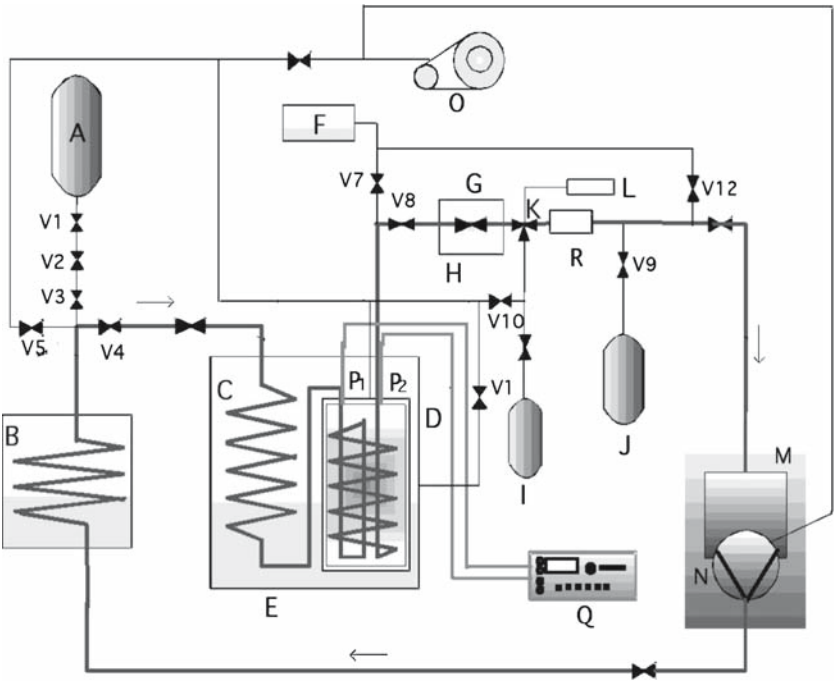

Fig. 1. Apparatus A: sample bottle, B: evaporator, C: heat exchanger, D: calorimeter, E: temperature controlled bath, F: pressure gauge, G: needle valve (expansion valve), H: temperature controlled bath, I: sampling cylinder, J: sub condenser, K: 3-way solenoid valve, L: timer, M: condenser, N: recirculation liquid pump, O: vacuum pump, P1: inlet platinum resistance thermometer, P2: outlet platinum resistance thermometer, R: mass flow meter. The sample flow (except when measuring the flow rate) is indicated by the bold line.

Part of the heating energy, $\dot{Q}_{\mathrm{L}}$, is released from the sample and the calorimeter to the surroundings even though the calorimeter is thermally shielded. In order to determine the value of $\dot{Q}_{\mathrm{L}}$, more than five $c_{p\mathrm{app}}$ data were measured by changing the mass flow rate from 0.018 to 0.082 g·s^{-1} with $\Delta T = 2$ K at the same temperature and pressure. By plotting $c_{p\mathrm{app}}$ vs. $1/\dot{m}$ and extrapolating the curve to $1/\dot{m} \to 0$, the actual c_p can be determined.

The sample pressure at the calorimeter outlet was measured with a precision quartz crystal pressure transducer (Paroscientific, Model 31K-101) (F).

2.2. Materials

A high-purity sample of R-143a was obtained for this study. The R-143a was certified by the manufacturer to have a minimum purity

of 99.95 mol% by gas chromatographic analysis. The sample fluid was filled into the apparatus from the sample cylinder. The total mass of the charged sample was about 1 kg.

2.3. Assessment of Uncertainties

The experimental expanded uncertainty according to the ISO guideline (with a coverage factor $k = 2$) of the temperature increment measurement is 25 mK, by considering the calibration test of the PRTs (the expanded uncertainty is 3.5 mK), the temperature distribution in the calorimeter, and the accuracy of each instrument. The uncertainty of the pressure measurement is 7 kPa, based on the pressure transducer's specifications (0.6 kPa) and pressure fluctuations (<3.5 kPa). The expanded uncertainty of c_p is estimated from a combination of the standard uncertainty of the mass flow rate for 1 min (<0.10 mg·s^{-1}), that of the supplied heat quantity (<70 μW), and that of the temperature increment (<40 mK). The resulting expanded uncertainty of c_p ranges from 9 to 32 J·kg^{-1}·K^{-1} which depends on the conditions of each measurement.

3. RESULTS

Figure 2 shows the $c_p - T$ diagram of the present measurements and the previous c_p data for R-143a which were obtained at Keio University by using the same apparatus. Vertical error bars in the figure indicate the uncertainties of the experimental data. The experimental c_p values and the expanded uncertainties are tabulated in Table I. Table II shows the previous 17 data by Mukoyama [1], Mukoyama et al. [2], Nakashima [3], Takei [4], Yasumoto and Watanabe [5], and Yasumoto [6]. The present c_p measurements and earlier data show reasonable behavior. The behavior of isobars and the saturation curve calculated by available equations of state (EOSs) which have been formulated by Outcalt and McLinden [7], Li et al. [8], and by Lemmon and Jacobsen [9] based on experimental thermodynamic property data, are also shown in Fig. 2.

Evaluations of the c_p measurements were made with values calculated with the available EOSs developed by Outcalt and McLinden [7], Li et al. [8], and Lemmon and Jacobsen [9], who did not have access to the present, and most of the earlier c_p measurements except for the data by Mukoyama et al. Therefore, these EOSs were developed without the gaseous c_p data measured on several isobars. Figures 3–5 show the relative deviations of the c_p measurements.

Figure 3 shows the c_p deviations of a modified Benedict-Webb-Robin (MBWR) equation of state developed by Outcalt and McLinden [7].

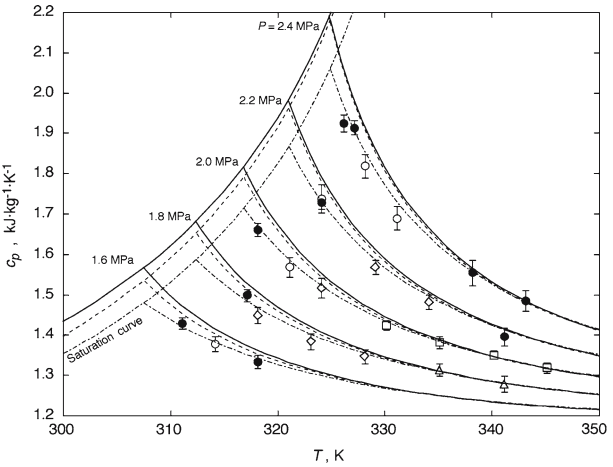

Fig. 2. Experimental measurements for the present and previous data. □: Mukoyama [1], Mukoyama et al. [2], △: Nakashima [3], ◇: Takei [4], ○: Yasumoto and Watanabe [5], Yasumoto [6], •: This work, ----: Outcalt and McLinden [7], —: Li et al. [8], - - - : Lemmon and Jacobsen [9].

Table I. Experimental c_p Results for R-143a from This Study

T (K)	p (MPa)	c_p (kJ·kg^{-1}·K^{-1})	Expanded uncertainty ($k = 2$)		
			T (mK)	p (kPa)	c_p (J·kg^{-1}·K^{-1}) (%)
311.15	1.6	1.430	18	4.3	9 [0.59]
318.15	1.6	1.330	8	7.7	14 [1.02]
317.15	1.8	1.498	20	4.6	16 [1.07]
318.15	2.0	1.660	25	2.9	17 [1.01]
324.15	2.2	1.729	15	4.5	16 [0.94]
341.15	2.2	1.395	15	5.9	21 [1.53]
326.15	2.4	1.924	16	5.4	24 [1.25]
327.15	2.4	1.913	22	6.9	12 [0.62]
338.15	2.4	1.554	21	4.5	32 [2.04]
343.15	2.4	1.485	11	5.0	20 [1.37]

Table II. Previous c_p Measurements for R-143a

T (K)	p (MPa)	c_p (kJ·kg^{-1}·K^{-1})
Mukoyama [1], Mukoyama et al. [2]		
330.15	2.0	1.424
335.15	2.0	1.381
340.15	2.0	1.350
345.15	2.0	1.318
Nakashima [3]		
335.16	1.8	1.313
341.17	1.8	1.278
Takei [4]		
318.15	1.8	1.448
323.15	1.8	1.384
328.15	1.8	1.346
324.15	2.0	1.516
329.15	2.2	1.567
334.15	2.2	1.481
Yasumoto and Watanabe [5], Yasumoto [6]		
314.15	1.6	1.377
321.15	2.0	1.568
324.15	2.2	1.737
328.15	2.4	1.818
331.15	2.4	1.689

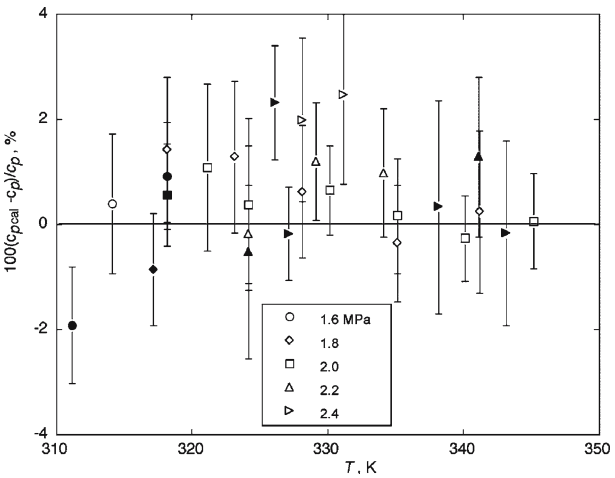

Fig. 3. Deviations of calculated values with an EOS by Outcalt and McLinden [7] for R-143a from the present (closed symbols) and previous (open symbols) c_p data.

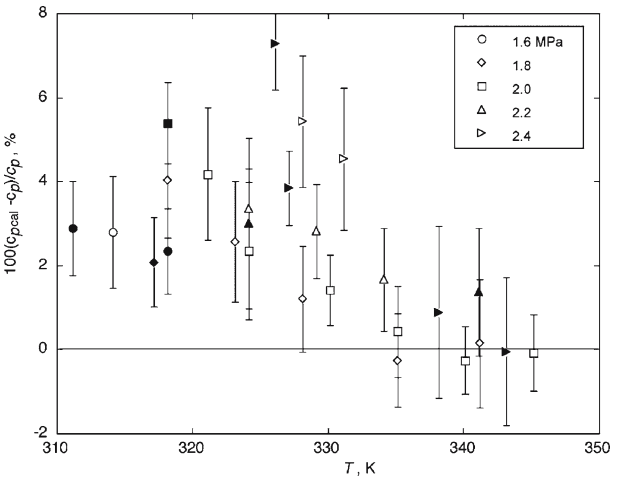

Fig. 4. Deviations of calculated values with an EOS by Li et al. [8] for R-143a from the present (closed symbols) and previous (open symbols) c_p data.

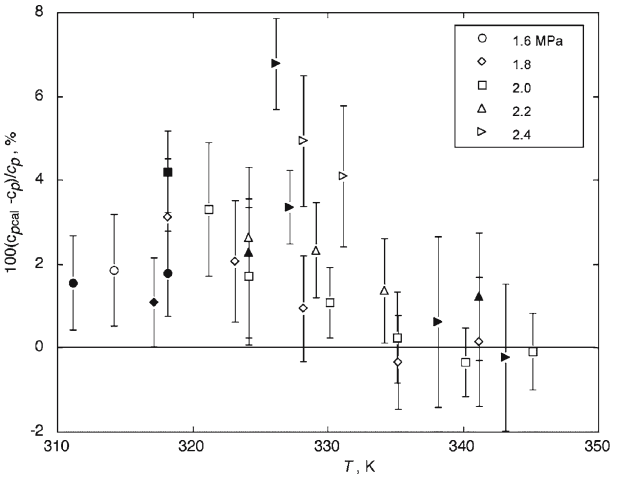

Fig. 5. Deviations of calculated values with an EOS by Lemmon and Jacobsen [10] for R-143a from the present (closed symbols) and previous (open symbols) c_p data.

Table III. Bias and Average Absolute Deviations (AAD) with Calculated Data from Available EOSs ($c_{p\text{cal}}$) and Present 10 Data Points and Earlier 17 Data Points (c_p)

EOS	$\text{Bias} = 100\frac{1}{N}\sum_{i=1}^{N}\frac{(c_{p\text{cal}}-c_p)}{c_p}$ (%)	$\text{AAD} = 100\frac{1}{N}\sum_{i=1}^{N}\frac{\lvert c_{p\text{cal}}-c_p\rvert}{c_p}$ (%)
Outcalt and McLinden [7][a]	0.51	0.84
Li et al. [8][b]	2.41	2.46
Lemmon and Jacobsen [9][b]	1.91	1.99
Span [10][b]	2.80	2.81
Sato et al. [11][c]	-0.13	0.78

[a] MBWR.
[b] Helmholtz.
[c] Virial.

The EOS presents the data within their uncertainties for most of the points.

Figure 4 shows the c_p deviations of an equation of state developed by Li et al. [8]. Good agreement of ±1% was noted above 335 K. At lower temperatures, the systematic deviations increase significantly. The deviations increase as the saturation curve is approached. This model is a Helmholtz-type equation.

Another Helmholtz-type model by Lemmon and Jacobsen represents the present data and the previous data (Fig. 5). These data are represented within ±2% except near the saturation line where the deviations increase to 4.2, 2.7, and 6.8% at 2.0, 2.2, and 2.4 MPa, respectively. The systematic deviations increase significantly at lower temperatures although these are slightly less than those for the EOS by Li et al. [8].

Table III shows the systematic and absolute c_p deviations of five available EOSs [7–11] with the present 10 data points and the earlier 17 data points. Among Helmholtz models for R-143a, the EOS proposed by Lemmon and Jacobsen represents the data well. The EOS by Span [10] shows a similar behavior as that by Li et al. A virial equation of state by Sato et al. [11] was formulated with published data of pressure–volume–temperature properties and speed of sound in the gas phase. The EOSs by Sato et al. and Outcalt and McLinden show small systematic and average deviations, with Sato et al. being the better representation. The three Helmholtz-type EOSs show larger systematic and average deviations of 1.91 to 2.81%. Among the equations, therefore, the best agreements with the c_p data are obtained by the virial equation.

4. CONCLUSIONS

Measurements of c_p were reported for R-143a in the gas phase. The available EOSs represent the observed behavior at most conditions with the exception of c_p near the saturation curve. At temperatures near the saturation curve, the calculations by the Helmholtz-type EOSs deviate from the c_p measurements by more than +2%. The MBWR and virial-type equations represent the data over the entire temperature range, but both have a slight systematic bias from the measurements, because the equations were not correlated to the data. These data will be essential to develop accurate models to represent thermodynamic properties of R-143a.

ACKNOWLEDGMENTS

The authors gratefully acknowledge Hiroyuki Miyamoto, Keio Univ., and Kouji Yasumoto and Tomoyuki Tanaka (graduated students of Keio Univ.) for their technical assistance on the project. Also, the authors acknowledge Kenichi Tamura, National Defense Academy, for the c_p measurements.

REFERENCES

1. K. Mukoyama, M. S. Thesis (Keio Univ., Yokohama, Japan, 1996) [in Japanese].
2. K. Mukoyama, H. Sato, and K. Watanabe, in *Proc. Int. Conf. High Press. Sci. Tech.*, M. Nakaiwa, ed. (Kyoto, 1998), p. 158.
3. A. Nakashima, M. S. Thesis (Keio Univ., Yokohama, Japan, 1998) [in Japanese].
4. A. Takei, M. S. Thesis (Keio Univ., Yokohama, Japan, 2000) [in Japanese].
5. K. Yasumoto and K. Watanabe, *Proc. 16th European Conf. Thermophys. Props.*, CD-ROM, (London, 2002).
6. K. Yasumoto, M. S. Thesis (Keio Univ., Yokohama, Japan, 2003) [in Japanese].
7. S. L. Outcalt and M. O. McLinden, *Int. J. Thermophys.* **18**:1445 (1997).
8. J. Li, R. Tillner-Roth, H. Sato, and K. Watanabe, *Int. J. Thermophys.* **20**:1639 (1999).
9. E. W. Lemmon and R. T. Jacobsen, *J. Phys. Chem. Ref. Data* **29**:521 (2000).
10. R. Span, *Multiparameter Equations of State – An Accurate Source of Thermodynamic Property Data* (Springer, Berlin, Heidelberg, New York, 2000).
11. H. Sato, N. Kagawa, Y. Takaishi, Y. Higashi, C. Yokoyama, K. Fujii, K. Murakami, M. J. Assael, and M. Noguchi, *Proc. Int. Refrig. Air Cond. Conf.*, CD-ROM (Purdue Univ., West Lafayette, Indiana, 2002).